Article

J. Biol. Regul. Homeost. Agents. 2024; 38(2): 913–924
https://doi.org/10.23812/j.biol.regul.homeost.agents.20243802.74

Decreased Resolvin D1 and Increased Fatty Acid Oxidation Contribute to Severity Score of Krabbe Disease in Twitcher Mice

Cinzia Signorini[1,*], Giulia Collodel[1], Giovanna Pannuzzo[2], Adriana Carol Eleonora Graziano[2], Elena Moretti[1], Daria Noto[1], Giuseppe Belmonte[1], Venera Cardile[2,*]

[1]Department of Molecular and Developmental Medicine, University of Siena, 53100 Siena, Italy
[2]Department of Biomedical and Biotechnological Sciences, Section of Physiology, University of Catania, 95123 Catania, Italy
*Correspondence: cinzia.signorini@unisi.it (Cinzia Signorini); cardile@unict.it (Venera Cardile)
Published: 1 February 2024

Background: Krabbe disease is due to a deficiency of lysosomal enzyme galactosylceramidase, which leads to destruction of the myelin sheath around nerves in the brain and spinal cord. In addition, Krabbe disease is associated with neuroinflammation in which harmful amounts of lipids are produced. To assess the importance of the regulation of lipid metabolism in the pathogenesis and intervention options in Krabbe disease, the aim of this study was to identify a set of specific biomarkers in a mouse model of the disease and to analyze the correlation between each biomarker.

Methods: In this study, fatty acid mediators were investigated in twitcher mice, a natural model of Krabbe disease, and the genotype was determined. Mass spectrometry was used to quantify F_2-isoprostanes and immune techniques were used to investigate F_2-isoprostanes, resolvin D1 (RvD1), peroxisome proliferator-activated receptor gamma, apelin, and the apelin receptor in the brains of heterozygous and affected homozygous mice and in wild-type control mice.

Results: The results of molecular analysis showed that there was a reduction in peroxisome proliferator-activated receptor gamma in the brains of both heterozygous and affected homozygous mice ($p < 0.001$). In addition, in the brains of mice with Krabbe disease RvD1 levels were decreased ($p < 0.001$), oxidation of arachidonic acid was increased ($p < 0.001$) and low levels of apelin ($p < 0.001$) were associated with an increase in apelin receptor ($p < 0.05$). RvD1 and apelin levels were associated with disease severity ($r = –0.638$, $p < 0.001$ and $r = –0.725$, $p < 0.001$, respectively).

Conclusion: Our results indicate that mutation of the galactosylceramidase gene is associated with altered homeostasis of fatty acid oxidative metabolism. These homeostatic alterations reflect the disease phenotype. Our findings highlight a relevant aspect of fatty acid metabolism in the Krabbe disease brain and support the view that fatty acid metabolism is an active player in the pathogenesis of this still incurable disease.

Keywords: apelin; neuroinflammation; isoprostanes; peroxisome proliferator-activated receptor gamma; resolvin D1; Krabbe disease

Introduction

Krabbe disease (KD) is an inherited neurological disorder that results from mutations in the galactosylceramidase (*GALC*) gene encoding lysosomal enzyme galactosylceramidase (GALC). Functional deficiency of GALC protein leads to destruction of the myelin sheath around nerves, both in the brain and spinal cord [1,2]. In addition, neuroinflammation and neuronal degeneration in the gray matter occur [3,4].

The association between neuroinflammation and functions of the central nervous system has been largely investigated in cognitive impairment [5,6]. In particular, neuroinflammation is observed in leukodystrophy diseases and is linked to white matter pathology and disease severity [3,7,8]. In addition, KD investigations were concerned with neuroinflammatory genes [3] and it has been reiterated that secondary neuroinflammation may occur together with psychosine-induced demyelination in KD [9].

Inflammatory mediators are widely involved in pathophysiology of different neuropsychiatric and neurodegenerative diseases and new therapeutic strategies are focused on them [10]. As a specific group of lipid mediators involved in inflammatory regulation, specialized pro-resolution mediators (SPMs) represent a class of cell signaling molecules mediating molecular signaling to resolve inflammation and to modulate tissue remodeling [11,12]. In particular, SPMs biosynthesized from docosahexaenoic acid (DHA), commonly known as resolvins (Rvs), are reported as anti-inflammatory and neuroprotective agents also capable of protection against the cellular damage induced by oxida-

Journal of
BIOLOGICAL REGULATORS
and Homeostatic Agents

tive stress [13–15]. Resolvin D1 (RvD1) is one of the most relevant Rvs [14,16]. SPMs are also derived from arachidonic acid (ARA) [16], a polyunsaturated fatty acid playing a relevant role for cell functions, including nervous system cells. Conversely, specific eicosanoids derived from ARA are recognized in contributing to the initiation of inflammation and chronic inflammation. Additional ARA metabolites are the oxygenated ones, known as F_2-isoprostanes (F_2-IsoPs) [17]. Assessment of bioactive eicosanoids has been highlighted as a promising analytical opportunity to study the eicosanoid function in inflammatory- and oxidative stress-related diseases [18]. Previously, F_2-IsoPs, as well as, F_2-dihomo-IsoPs (whose precursor fatty acid is the adrenic acid) and F_4-neuroprostanes (whose precursor fatty acid is DHA) have been shown to be relevant to KD severity [19].

Interestingly, peroxisome proliferator-activated receptor gamma (PPARγ), as a nuclear receptor particularly involved in the modulation of lipid oxidation and inflammatory response, represents a link between the two pathological processes (inflammation and lipid peroxidation) [20].

Apelin receptor (APJ), an endogenous ligand for the G protein-coupled receptor, is widely distributed within the central nervous system and apelin/APJ is involved in inflammatory response modulation [21]. Neuroprotective roles of apelin have been described in Alzheimer's disease [22], and the role of apelin/APJ axis in the pathogenesis of Parkinson's disease appears to be relevant [23]. Additionally, low serum apelin levels have been found to be associated with mild cognitive impairment in Type 2 diabetes [24]. Interestingly, the association between apelin/APJ, oxidative stress and inflammation-related diseases has been examined [25]. Moreover, the apelin/APJ system has been reported [26] to be correlated with energy metabolism, including glucose tolerance, insulin sensitivity [27], respiratory diseases [28], and appetite and drink behavior [29,30].

Here, as information relevant to the progression of KD pathogenesis, we examined the inflammatory response and lipid metabolism in the brain of KD mice (a well-established animal model of the disease). A panel of specific biomarkers (i.e., RvD1, F_2-IsoPs, PPARγ, apelin, and APJ) were examined (i.e., quantified and immunolocalized) and found to be interrelated. All evaluations were performed in both heterozygous mice (carriers of the *GALC* gene mutation) and homozygous twitcher mice (according to genotype determinations) and in wild-type control mice.

Materials and Methods

Animals

The animals, pairs of twitcher heterozygous mice, a strain that contains a premature stop codon (W339×) in the *GALC* gene that inhibits enzymatic activity, were housed in plastic cages in our facility at the Department of Biomedical and Biotechnological Sciences (University of Catania) and were given standard granulated feed and tap water ad libitum. The twitcher mouse is a naturally occurring model of human KD. The biochemical and neuropathological findings in twitcher closely resemble that observed in humans with KD. Since it closely mimics the human disorder, the twitcher mouse has become a valuable model not only to understand the pathogenesis of Krabbe disease, but also to develop strategies to correct the galactocerebrosidase deficiency [31]. For our study, pairs of mice carrying the mutation of the *GALC* gene were crossed repeatedly in order to obtain a progeny of twitcher mice. The probability of generating diseased mice is 25% (among 4 puppies, 1 is a diseased mouse) for each progeny for which animals affected by Krabbe belong to different litters. The Institutional Animal Care and Use Committee approved all experimental procedures involving animals in accordance with institutional guidelines for animal care and use (Project no. 364; authorization no. 61/2022-PR).

Genotyping

The genotypes were determined by high resolution melting (HRM) analysis. The genomic DNA of 10–12 days old pups born from twitcher heterozygotes was extracted from clipped tails according to the method provided by the kit manufacturer (REDExtract-N-Amp™ Tissue PCR Kit: Extraction Solution, cat. E7526, Tissue Preparation Solution, cat. T3073, and Neutralization Solution B, cat. N3910, Merk, Sigma Aldrich, Milan, Italy) [19]. Genomic DNA was amplified according to the manufacturer's protocol of Type-it HRM PCR kit (Cat. No. 206544, Qiagen, Instrumentation Laboratory, Milan, Italy) using the following specific primers: 5′-ATCAGACTGAAATTGGTAGACAGC-3′ for forward and 5′- GCCATCAGTCAGAGCAACATAAC-3′ for reverse. The analysis was performed on a Rotor-gene Q real-time analyzer (Rotor-Gene Q 2plex with HRM, Corbett, Qiagen, Milan, Italy).

Collection of Animal Brain Samples

In the life cycle of Krabbe-affected mice, clinical symptoms develop at the onset of the active myelination period and, if untreated, affected mice die at 35 ± 2 days. Therefore, for the brain and blood collection the sacrifice was selected on the 35th day (postnatal day P35, terminal course of the disease). Both males and females were used. Mice were sacrificed with CO_2 and then the brains were removed and immediately stored at –80 °C until further experiments. The following animals were used for the experiments:

1th group: 15 twitcher mice (8 males and 7 females);

2nd group: 15 heterozygous mice (7 males and 8 females);

3rd group: 15 healthy mice (9 males and 6 females).

Apelin Immunoassay

Whole brain tissue was homogenized (10% w/v) in PBS (pH 7.4) and apelin quantification carried out by sandwich quantitative enzyme-linked immunosorbent assay (Abbexa, Cambridge, UK, Catalog No: abx585113). The intensity of the color developed by the enzyme reaction was evaluated spectrophotometrically (wavelength; 450 nm). Determination of apelin amounts was performed by comparing the optical density of each brain tissue sample to the standard curve (constructed using known apelin amounts) ranging from 125.00 to 8000 pg/mL. In each sample, apelin measurement was performed in duplicate. Apelin levels were reported as pg/g brain tissue.

Indirect Immunofluorescence (IIF) Analysis

Brains of heterozygous and homozygous mice and wild-type control were dissected out and tissue sections of a thickness of 4 µm were prepared [32] and were treated with 10% buffered formalin for 24 h at 4 °C. Subsequently, brain sections were then washed in water for 1 h. After fixation, the tissues were dehydrated in a series of ethanol solutions (50%, 75%, 95%, and 100%) and cleared with xylene. The specimens were treated with three infiltrations of molten paraffin at 60 °C for 1 h and then solidified at room temperature. The blocks thus obtained were sectioned using a Leica RM2125 RTS microtome (Leica RM2125, Leica Biosystem, Wetzlar, Germany); coronal sections (4 µm) were collected in glass slides and stained using the hematoxylin-eosin method for routine histology. The paraffin sections, three different blocks from each brain tissue of the control and mutant mice, were deparaffinized with xylene and then treated in a series of ethanol concentrations (100%, 90%, 80%, and 70%) for 5 min and, finally, in water to rehydrate the tissue. For antigen retrieval, the sections were washed and treated with heat-induced epitope retrieval 1 (HIER 1) buffer (10 mM sodium citrate) at pH 6 for 20 min at 95 °C. Specimens were treated overnight at 4 °C with rabbit polyclonal anti-8-iso-$PGF_{2\alpha}$ antibody (ab2280, Abcam, Cambridge, UK) diluted 1:100, with monoclonal mouse anti-PPARγ (E-8) antibody FITC-conjugated (sc-7273, Santa Cruz Biotechnology, Inc., Dallas, TX, USA) at a dilution of 1:50, with rabbit polyclonal anti-apelin antibody (ab59469, Abcam, Cambridge, UK) diluted 1:200 and with rabbit monoclonal anti-APJ antibody (5H5L9, Invitrogen, Thermo Fisher Scientific, Waltham, MA, USA) diluted 1:100. After three washes for 10 min with PBS, the slides were treated with anti-8-iso-$PGF_{2\alpha}$, anti-apelin and anti APJ antibodies incubated with an anti-rabbit antibody raised in goat AlexaFluor® 488 conjugate (RRID: AB_143165, Invitrogen, Thermo Fisher Scientific, Carlsbad, CA, USA), diluted at 1:100 for 1 h at room temperature. Incubation in primary antibody was omitted in wild-type control samples. The slides were washed with PBS three times; then, nuclei were stained with 4',6-diamidino-2-phenylindole (DAPI) solution (GTIN 00884999021624, Vysis, Downers Grove, Italy). Slides were washed and mounted with 1,4-diazabicyclo(2.2.2) octane (DABCO, Product Number: 290734, Sigma-Aldrich, Milan, Italy) and analyzed with Leica DMI 6000 Fluorescence Microscope (Leica DMI 6000, Leica Microsystems, Wetzlar, Germany), the objective used to acquire the images was 63X, and the images were acquired by Leica AF6500 Integrated System for Imaging and Analysis (Leica AF6500, Leica Microsystems, Wetzlar, Germany). For standardization and comparison of the different groups, only good quality sections at the same magnification were investigated; at least 20 sections of tissue from each group were evaluated. One hundred cells in the cortex were selected using the nucleus/cytoplasm ratio as the selection criterion. The same operator evaluated three conditions: almost absent, limited and intense signal. These criteria were previously used in our lab for murine models of Rett syndrome [32] and for additional different cell samples [33].

RvD1 Immunoassay

In whole mouse brain tissue (brain tissue samples homogenized 10% w/v in PBS, pH 7.4), RvD1 amounts were measured by a double antibody sandwich technique and a biotin-labeled antibody and horseradish peroxidase-avidin conjugate were used (Catalog # MBS2601295, MyBioSource, San Diego, CA, USA). Spectrometric detection of color intensity at 450 nm allowed the quantification of RvD1 amounts by comparison to a standard curve (ranging from 2000 pg/mL to 31.2 pg/mL). Data were reported as pg/g brain tissue.

F_2-IsoP Determination in Mouse Brain

Currently, F_2-IsoPs are mainly generated by free radical-initiated peroxidation of esterified ARA in membrane. Thus, F_2-IsoPs, initially formed in situ on phospholipids (esterified F_2-IsoPs), are released into the circulation as unesterified F_2-IsoPs (free F_2-IsoPs) [34,35]. F_2-IsoPs were previously reported to be relevant to cerebral disease [36]. Here, in whole mouse brain tissue, total (sum of esterified and free) F_2-IsoPs were measured by gas chromatography/negative ion chemical ionization tandem mass (GC/NICI-MS/MS) (Trace GC and PolarisQ Ion Trap, Thermo Finnigan, San Jose, CA, USA), as previously performed [19]. Briefly, to an aliquot (1 mL) of brain homogenate aqueous KOH (1 mM, 500 µL) was added. After incubation at 45 °C for 45 min, the solution was acidified by adding HCl (1 mM, 500 µL). Each sample was spiked with 500 pg tetradeuterated prostaglandin $F_{2\alpha}$ ($PGF_{2\alpha}$-d_4) (Item No. 316010, Cayman Chemical, Ann Arbor, MI, USA), as an internal standard, and ethyl acetate (10 mL) was also added to extract total lipids. The total lipid extract was applied onto an NH_2 cartridge (Sep-Pak® Vac NH_2, 500 mg, WAT054560, Waters, Milford, MA, USA) and F_2-IsoPs were eluted. Subsequently, two derivatization processes were carried out. Firstly, the collected elu-

Journal of
BIOLOGICAL REGULATORS
and Homeostatic Agents

ates were incubated at 40 °C for 45 min, in the presence of pentafluorobenzyl bromide, 40 µL, 10% in acetonitrile, (N° CAT. 101052, Sigma-Aldrich, Milan, Italy); lastly, incubation at 45 °C for 1 h was performed in the presence of 50 µL of N,O-bis (trimethylsilyl)trifluoroacetamide, 10% in acetonitrile, (N° CAT.15222, Merck, Sigma-Aldrich, Milan, Italy). Subsequently, GC/NICI-MS/MS F_2-IsoP analyses were carried out. In all determinations, the measured ion was the product ion at *m/z* 299 produced from 15-F_{2t}-IsoP, one of the most represented isomers of F_2-IsoPs (also referred to as 8-Isoprostane, or 8-epi $PGF_{2\alpha}$). To quantify the amount of F_2-IsoPs in each test sample, a curve-fitting method was applied to generate the standard curve of the reference standard 15-F_{2t}-IsoP (Item No. 16350, Cayman Chemical, Ann Arbor, MI, USA).

Statistical Analysis

To assess normality of data the D'Agostino-Pearson normality test was applied. Multiple comparisons were carried out by one-way analysis of variance (ANOVA) with the Tukey post hoc test or the Kruskal-Wallis test followed by the nonparametric Mann-Whitney test or Dunn's multiple comparisons test, as appropriate. The association between variables were tested using the Spearman rank correlation at 95% confidence intervals (95% C.I.). A two-tailed $p \leq 0.05$ was considered to indicate statistical significance. The Graph-Pad Prism 8.0.0 statistical software package (Graph-Pad Software, Boston, MA, USA) was used for the data analysis.

Results

RvD1 in KD Brain

A significantly reduced concentration of RvD1 in brain tissue of the twitcher mice was found compared to wild type and heterozygous mice. In mice, brain levels of RvD1 were significantly different when wild type, heterozygous and twitcher mice were compared (Kruskal-Wallis, df = 2, H = 18.84; $p < 0.0001$; n, 45). In particular, brain amounts of RvD1 were shown to decrease according to the mice phenotype where it was found to be in the following order: twitcher < heterozygous = wild type. As reported in Fig. 1, RvD1 brain levels were significantly higher in wild-type mice as compared to the twitcher ones (n = 15 in each group; U = 22; $p < 0.0001$ by the nonparametric Mann-Whitney test) and were also significantly reduced in twitcher mice as compared to heterozygous mice (n = 15 in each group; U = 33; $p = 0.0006$ by the nonparametric Mann-Whitney test).

When a statistical comparison was carried out between heterozygous and wild type mice, no significant difference was found.

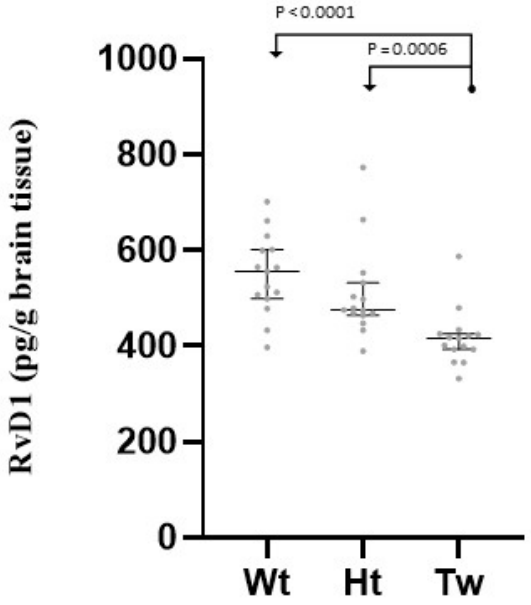

Fig. 1. Dot plots of resolvin D1 (RvD1) brain levels in wild-type, heterozygous and twitcher mice. The differences between the groups were compared using the nonparametric Kruskal-Wallis test followed by the nonparametric Mann-Whitney test. The horizontal lines represent the medians and the error bars represent 95% interquartile range. Description of the statistical results is reported in the text. The number of animals was n = 15 for each group. Legend: Wt, wild-type; Ht, heterozygotes; Tw, twitcher.

Apelin in KD Brain

As a relevant molecule in cognitive impairment and inflammatory response, apelin was tested in brain samples from wild type, heterozygous and twitcher mice and statistical significance was interpreted (Kruskal-Wallis, df = 2, H = 28.33; $p < 0.0001$; n, 45). Apelin was significantly higher in the wild-type mice compared to twitcher mice (n = 15 for each group; U = 10.5; $p < 0.0001$ by the nonparametric Mann-Whitney test), and to heterozygous mice (n = 15 in each group; U = 31; $p = 0.0004$ by the nonparametric Mann-Whitney test). Furthermore, heterozygous and twitcher mice showed significant differences for apelin in brain (n = 15 in each group; U = 16; $p < 0.0001$ by the nonparametric Mann-Whitney test) (Fig. 2).

Correlation of RvD1 and Apelin to F_2-IsoP Brain Levels

Brain levels of F_2-IsoPs were measured (median values, ng/g: 5.8, 7.1, and 23.8 in wild type, heterozygous and twitcher mice, respectively) and found to be inversely correlated to RvD1 levels (r = –0.635; 95% C.I.: –0.786 to –0.412; n = 45; $p < 0.001$). Brain levels of F_2-IsoPs were also correlated to apelin brain amounts (r = –0.579; 95% C.I.: –0.749 to –0.335; n = 45; $p < 0.001$). These results in-

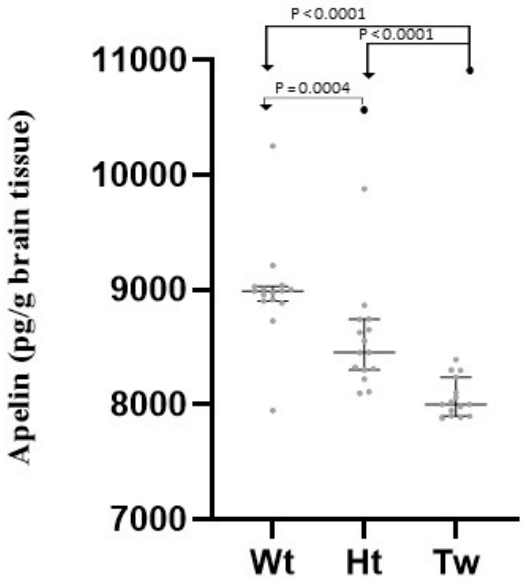

Fig. 2. Dot plots of apelin levels in brains of wild-type, heterozygous and twitcher mice. The differences between the groups were compared using the nonparametric Kruskal-Wallis test followed by the nonparametric Mann-Whitney test. The horizontal lines represent the medians and the error bars represent 95% interquartile range. Description of the statistical results is reported in the text. The number of animals was n = 15 for each group. Legend: Wt, wild-type; Ht, heterozygotes; Tw, twitcher.

dicated that increased oxidative lipid damage was concomitant both with reduction of neuroprotective role of apelin and resolution of inflammation by RvD1.

Correlation of RvD1 and Apelin to KD Severity Score

For each animal, the disease severity was quantified, according to the scoring criteria [19]. In particular, in twitcher mice the assigned phenotype score ranged from 1 (when main phenotypic features were: slight tremor, normal feeding, almost normal gait) to 3 (when main phenotypic features were: uncoordinated movements, severe tremor, paresis of the hind limbs, weight loss). Both wild type and heterozygous mice were healthy with a regular weight increase. Thus, each control and heterozygous mice were scored 0 (normal feeding, normal gait, and no signs of disease were present).

Brain levels of both RvD1 and apelin were significantly correlated to the phenotypic score. Brain levels of RvD1 were negatively correlated to the disease severity score (r = –0.638; 95% C.I.: –0.787 to –0.416; n = 45; $p < 0.001$), as well as apelin was (r = –0.725; 95% C.I.: –0.843 to –0.542; n = 45; $p < 0.001$) (Fig. 3). Significant positive relationships were observed between brain levels of RvD1 and apelin (r = 0.578; 95% C.I.: 0.335 to 0.749; n = 45; $p < 0.001$).

Thus, RvD1 and apelin are shown to be intimately associated in the molecular pathway of brain regeneration and to be intimately involved in KD disease progression.

F_2-IsoPs, PPARγ, Apelin, and APJ Immunolocalization in KD Brain

Immunocytochemistry examination of cortex brain cells showed that the signal of F_2-IsoPs inside the cytoplasm was intense in about 9% (9.3 ± 1.5) of the cells from wild-type control mice (Fig. 4A), in about 65% (65 ± 4.6) of the cells examined in brain section of homozygous mice (Fig. 4C), and in 30% (30 ± 2) of the cells in heterozygous mice (Fig. 4B). Intense fluorescent signal for F_2-IsoPs was significantly different when wild type, heterozygous and twitcher mice were compared (Kruskal-Wallis, df = 2, H = 7.2; $p = 0.0036$; n, 9). Thus, 2/3 of the cells observed showed an intense fluorescent signal in homozygous mice, while in wild-type control animals, only a few cells highlighted a positive signal for F_2-IsoPs (number of comparisons each family = 3; Z = 2.683; $p = 0.0219$, by Dunn's multiple comparisons) (Table 1). After incubation with PPARγ antibody, the cytoplasmic localization of the label was highly detectable in controls (about 64%, Fig. 4D), while it was almost absent in both heterozygous and homozygous mutant mice (Fig. 4E,F, respectively), in which half of the analyzed cells in the examined sections showed a limited extent of fluorescence. The extent of the absence of fluorescent signal for PPARγ was significantly different when wild type, heterozygous and twitcher mice were compared (Kruskal-Wallis, df = 2, H = 6.489; $p = 0.010$; n, 9) and the wild-type control group was significant different as compared to twitcher mice (number of comparisons each family = 3; Z= 2.534; $p = 0.0338$, by Dunn's multiple comparisons) (Table 1).

The immunofluorescent signal of apelin was intense in the brain of wild-type mice (Fig. 5), thus confirming quantitative determination displayed in Fig. 2. As a whole, our data on apelin supports a derangement of neuroprotection mechanisms, which are known to act in avoiding neuronal damage and impairment of neurologic function.

As further data on apelin/APJ receptor, immunofluorescent detection of APJ was carried out (Fig. 6). In homozygous twitcher mice, a major presence of the apelin receptor was evidenced. Such data confirms, together with immunodetection of apelin (Fig. 5), the derangement of the apelin/APJ system as a relevant feature in KD pathophysiological pathway. In particular, in the brain of homozygous twitcher mice the immunofluorescent signal of APJ is increased, whereas the apelin signal is reduced. Both in APJ and apelin immunofluorescent detection, the percentage of cells with increased (APJ detection) or decreased (apelin detection) fluorescent signal was significantly different in homozygous twitcher mice as compared to wild-type control mice ($p < 0.05$). In all experiments for immune detection, the analysis of the cortex cells in the examined sec-

Journal of
BIOLOGICAL REGULATORS
and Homeostatic Agents

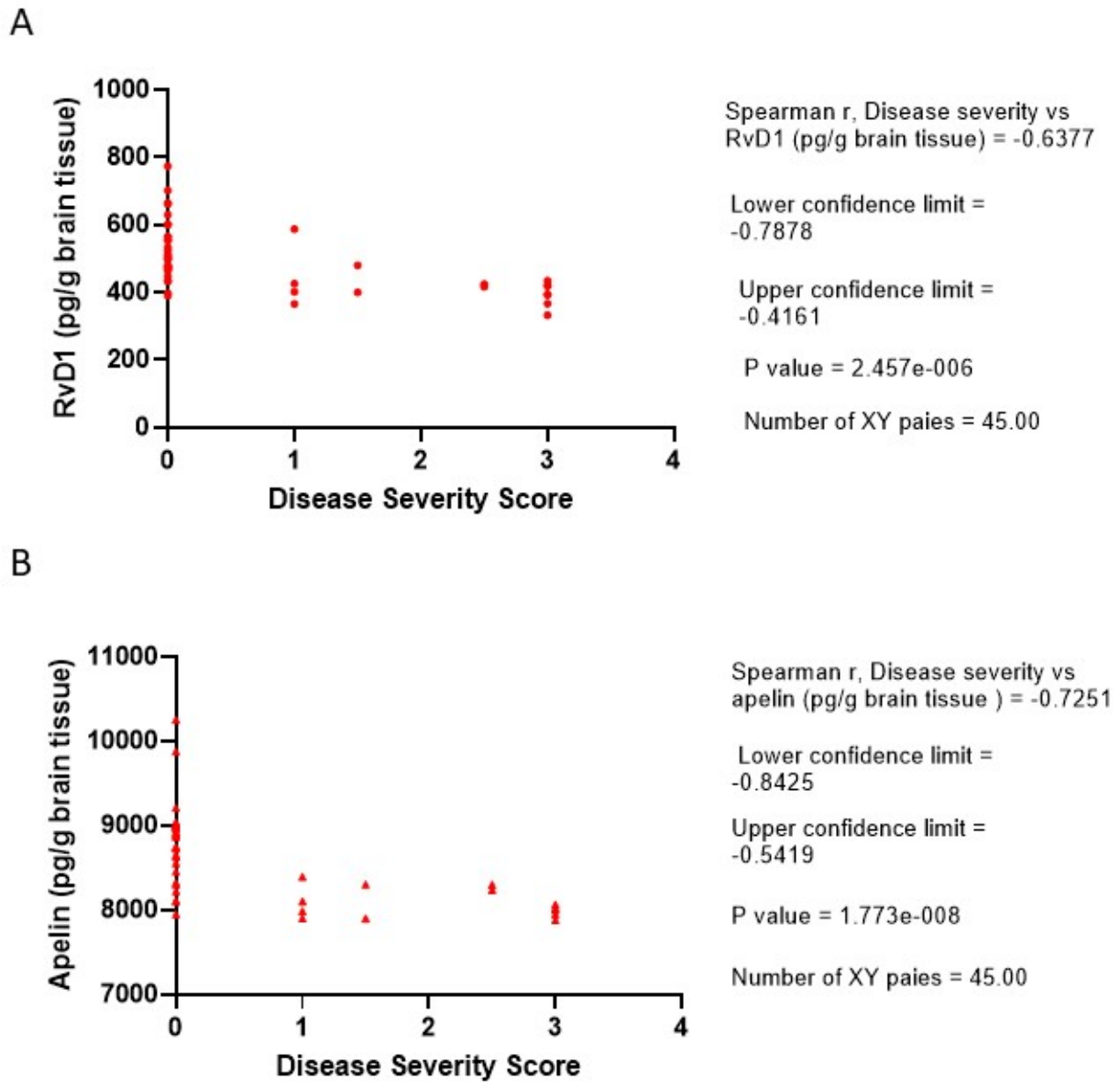

Fig. 3. Relationship between resolvin D1 (RvD1) and apelin levels in brain tissue and disease severity. (A) Scatter diagram for brain tissue RvD1 levels and disease severity. (B) Scatter diagram for brain apelin levels and disease severity. The relationship between the variables was tested using the Spearman correlation test. The Spearman coefficient, the lower and upper limits of the 95% confidence intervals, the number of data pairs and the *p*-values are shown. The phenotype score ranges from 0.0 to 3.0. In the study, each animal was assigned a value of 0.0, 1.0, 1.5, 2.5 or 3.0 depending on the phenotypic traits. A higher score meant a higher severity of the disease. Several animals had the same severity. ● and ▲ stand for RvD1 (A) and apelin (B) data.

tions was performed according to the standardization and comparison procedures described in Material and Method.

Discussion

We demonstrated here that nonresolving inflammation, increased fatty acid oxidation, and impaired lipid metabolism were associated with severity of KD. Our results highlight a relevant aspect of fatty acid metabolism in brain neuropathophysiology and support the view that fatty acid metabolism is an active player in the pathogenesis of KD. Modulation of inflammation and lipid metabolism in the brain could improve quality of life in KD.

There is increasing evidence that inflammation is a common biological mechanism in neurodegenerative diseases in which homeostasis is destabilized [37].

Certainly, neuroinflammation could represent the triggering factor of neuropathology, although it is secondary to

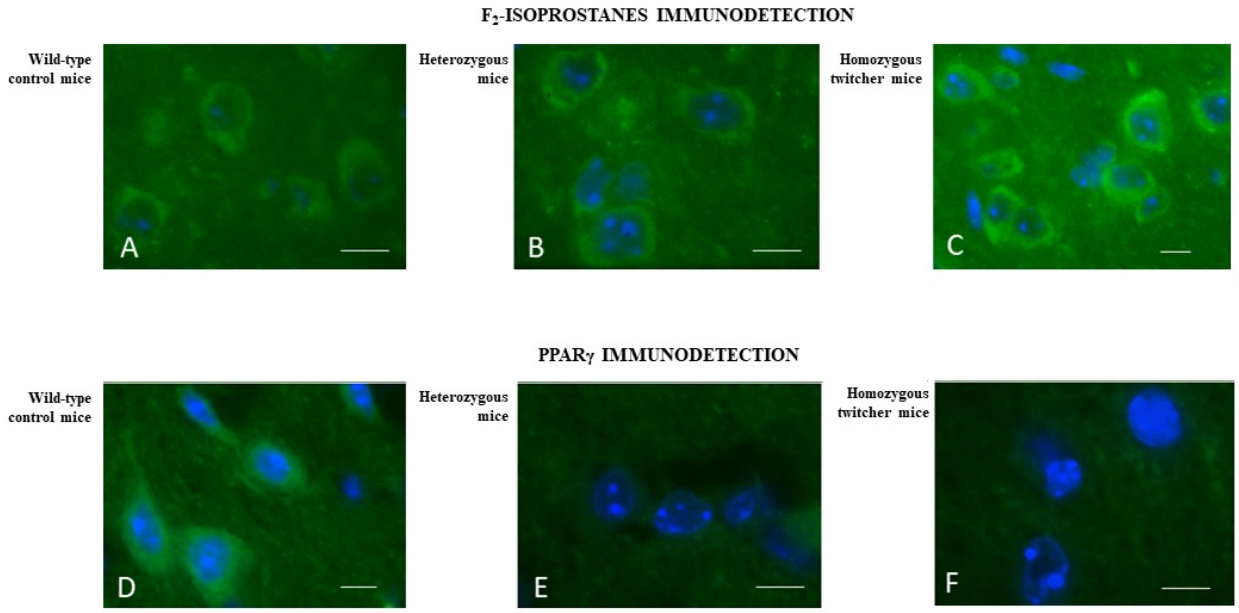

Fig. 4. Indirect immunofluorescence microscopy for F_2-isoprostanes (F_2-IsoPs) (A–C) and peroxisome proliferator-activated receptor gamma (PPARγ) (D–F) in wild-type control mice, heterozygous mice and homozygous twitcher mice. Representative brain sections from wild-type control, heterozygous and homozygous mice incubated with polyclonal anti-F_2-IsoPs (A–C, respectively) and anti-PPARγ antibodies (D–F, respectively). The nuclei were identified by counterstaining with the nuclear marker 4',6-diamidino-2-phenylindole (DAPI). The immunolocalization of F_2-IsoPs showed in the cytoplasm a faint fluorescent stain in control (A); the signal was more evident in heterozygous (B) mice. A high intensity signal was evident in the brain from the homozygous twitcher mice (C). The label after incubation with anti PPARγ antibody appeared intense in the control brain (D) and completely absent in brains from mutant mice (i.e., heterozygous mice, (E) and homozygous twitcher mice, (F)). The name of each animal group is given on the left side of each picture box. Scale Bar: 30 μm.

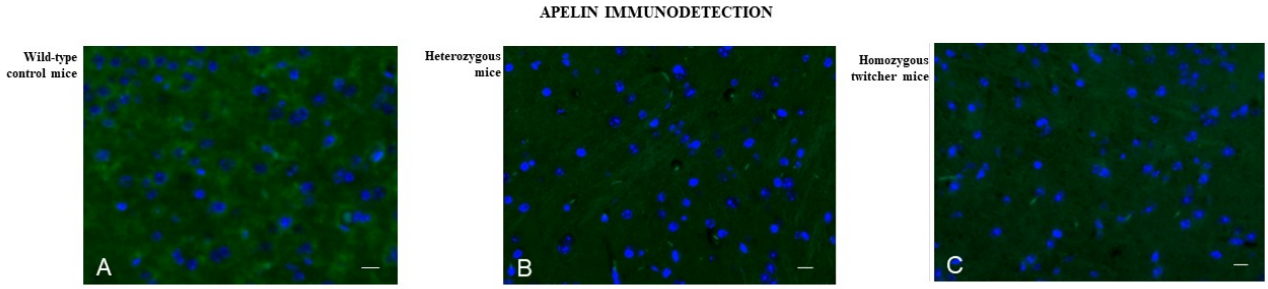

Fig. 5. UV micrographs of mouse brain from wild-type control mice (A), heterozygous mice (B) and homozygous twitcher mice (C) treated with an anti-apelin antibody. Representative brain sections from wild-type control, heterozygous and homozygous mice incubated with polyclonal anti-apelin antibody. The nuclei were identified by counterstaining with the nuclear marker DAPI. Increased apelin immunofluorescence signal was detected in the brain of wild-type mice (A). The name of each animal group is given on the left side of each picture box. Scale Bar: 30 μm.

genetic-environmental cause (i.e., Alzheimer and Parkinson diseases). In addition, neuroinflammation could represent the mechanism responsible for the progression of the disease, even though the latter was primarily triggered by genetic causes. With reference to KD, the transcriptional expression of Interleukin 1 beta, but not the related family member Interleukin 18, was shown to be upregulated in the brain stem and spinal cord of twitcher mice. Intriguingly, the maximal transcription of Interleukin 1 beta occurs in the pre-symptomatic and early symptomatic stage and not at the final stage of the disease. Thus, in KD pro-inflammatory signal is intimately related to the pathogene-

Journal of
BIOLOGICAL REGULATORS
and Homeostatic Agents

Table 1. Percentage of cells in the examined sections showing F_2-isoprostanes (F_2-IsoP) and peroxisome proliferator-activated receptor gamma (PPARγ) cytoplasmic signal in cortex brain of wild-type control and mutant mice.

Fluorescent signal in immunolocalization	Wild-type		Heterozygous		Homozygous	
	F_2-IsoP positive cells (%)	PPARγ positive cells (%)	F_2-IsoP positive cells (%)	PPARγ positive cells (%)	F_2-IsoPs positive cells (%)	PPARγ positive cells (%)
Almost absent signal	13.6 ± 2.5	7.7 ± 1.5	11.3 ± 2.1	21.6 ± 3.1	13.66 ± 3.2	30 ± 4.3*
Limited fluorescent signal	66.3 ± 3.1	24 ± 2.6	44 ± 4	61 ± 7.5	10.66 ± 2.1	57 ± 3
Intense fluorescent signal	9.3 ± 1.5	64 ± 4.6	30 ± 2	1.48 ± 1.5	65 ± 4.6**	1.12 ± 1

Data are expressed as mean values ± SD and are referred to the three most representative assays. The differences in fluorescent signal levels between the investigated groups were compared using Kruskal-Wallis test followed by Dunn's multiple comparisons test. Legend: ** $p = 0.02$, F_2-IsoP, positive cells with intense fluorescent signal, homozygous mice as compared to wild-type control mice; * $p < 0.05$, PPARγ, cells with almost absent fluorescent signal homozygous mice as compared to wild-type animals. Detailed statistical data are shown in Results. Number of sample, n = 9, for each detected parmeter.

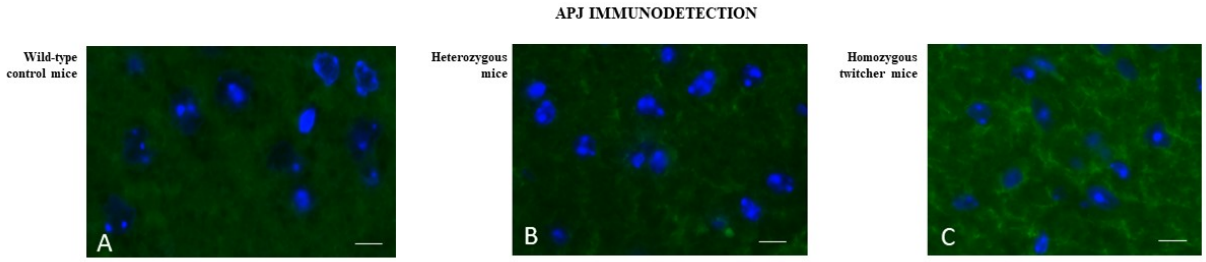

Fig. 6. UV micrographs of mouse brain from wild-type control mice (A), heterozygous mice (B) and homozygous twitcher mice (C) treated with an anti-apelin receptor (APJ) antibody. Representative brain sections from wild-type control, heterozygous and homozygous mice incubated with polyclonal anti-APJ antibody. The nuclei were identified by counterstaining with the nuclear marker DAPI. A pronounced presence of the apelin receptor was detected in homozygous twitcher mice (C). The name of each animal group is given on the left side of each picture box. Scale Bar: 30 µm.

sis of the disease [38]. As a relevant matter, the balance between pro-inflammatory and anti-inflammatory mediators is involved in defining the outcome after injury. Since in the inflammatory process the fine regulation of the resolution phase determines cell regeneration and wound healing, or progression of the inflammatory response, the alteration of the inflammation resolution step can lead to progressive organ dysfunction. With reference to neuropathic conditions, altered sympathetic and/or vagal tone are associated with a higher risk of chronic inflammatory disorders [39]. Thus, molecules and mechanisms enrolled in regulation of inflammatory response represent potential targets in therapeutic strategy development [40]. Interestingly, lipid mediator class switching occurs during regulation of inflammation [13,41].

Among SPMs accelerating resolution of acute inflammation, the D-series resolvins (including RvD1) are derived, as well as the neuroprotectins and the maresins, from DHA [42,43]. DHA, which performs several function in the central nervous system (mainly, cell survival, neuronal morphology, synaptic function, ion channel modulation, plasma membrane integrity and activity against disease) [44], was previously found to be under oxidative stress and non-enzymatic oxidation in twitcher mice [19]. Notably, in patients affected by Alzheimer's disease a reduced release of pro-inflammatory cytokines was detected after supplementation with a DHA-rich diet and high levels of brain DHA are linked to reduced expression of pro-inflammatory cytokines in several rodent models of acute or chronic neuroinflammation [45]. In addition, in the central nervous system, pathological conditions (also including neurodegenerative diseases) evidence connecting brain DHA and ω-3 PUFA levels were found [44]. Thus, modulation and regulation of DHA levels and metabolism could represent new therapeutic approaches in the management of brain diseases. Furthermore, RvD1 itself has been shown to be responsible for neurofunctional recovery and neuroprotection once administered *in vivo* [46]. Moreover, in an animal model of a diet rich in corn oil the impairment of memory function and hippocampal damage were induced by the decrease of RvD1 and prevented by the administration of RvD1 [47].

When making specific reference to neurodegenerative disorders, in Alzheimer's disease RvD1 was shown to stim-

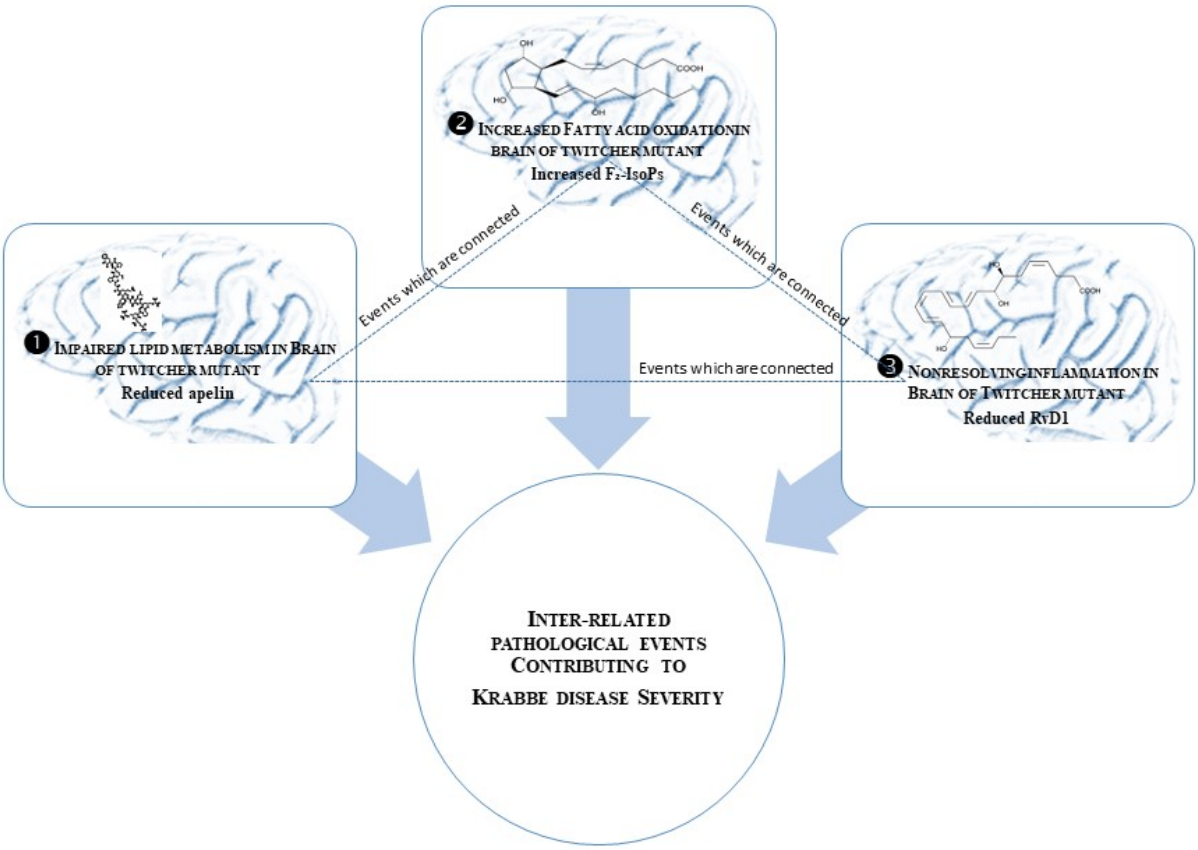

Fig. 7. Nonresolving inflammation and impaired lipid metabolism in the brain are connected and related to Krabbe disease severity. Reduced brain amounts of peroxisome proliferator-activated receptor gamma (PPARγ) represent the first step of the deranged lipid metabolism, also evident in asymptomatic heterozygous animals. In symptomatic twitcher mice, the impaired lipid metabolism causes alteration to production of apelin❶ and induces increased F_2-isoprostanes (F_2-IsoP) levels❷ and reduced amounts of resolvin D1 (RvD1)❸. Drawing software, PowerPoint 2013 (Microsoft Office Professional Plus 2013, Redmond, WA, USA).

ulate phagocytosis of amyloid-β by rebalancing inflammation and the reduced intake of DHA was suggested to contribute to the pathology [48]. In addition, RvD1 administration was shown to prevent neuroinflammation, neuronal dysfunction, and motor deficits in a rat model of Parkinson's disease [49].

In our study, a novelty is represented by the detection of a specific specialized pro-resolving lipid mediator that is known to be involved in regulation of the resolution of inflammation [12]. Here is shown that an impaired formation of RvD1 appears to be intimately and proportionally (as referred to the condition of heterozygosis or homozygosis, in the comparison of twitcher vs heterozygous mice) involved in the pathological mechanisms of KD as the levels of RvD1 are significantly low in twitcher mice in which the typical symptoms of the disease are present. Our data on RvD1 and reduced resolution of inflammation are consistent with the concurrent finding of PPARγ reduction in KD, as it was previously hypothesized that reduced PPARγ activation may contribute to chronic brain inflammation [50]. Thus, a relevant role for neuroinflammation in KD is confirmed [51] and an inflammatory unbalance is suggested. In particular, a role for RvD1 in detecting defective control of the inflammatory process is proposed. Accordingly, approaches to the resolution or modulation of inflammation represent emerging insights into the homeostatic network in which the inflammatory response is involved [52].

Apelin is widely expressed in the central nervous system and has been investigated in psychosis and neuropathy. In particular, for apelin a regulatory effect on memory and epilepsy, a protective role against memory impairment, and the presence in the hippocampus, amygdala, and cerebral cortex, areas known to be closely related to learning and memory, have been reviewed [53]. Here, low levels of apelin are identified in association with the clinical manifestation of neurological symptoms to trace the deficiencies in neurological functions. Interestingly, since endogenous apelin is required for the suppression of inflammation-induced vascular hyperpermeability [54], in our study the concomitant reduction of apelin and RvD1 confirm a lack

Journal of
BIOLOGICAL REGULATORS
and Homeostatic Agents

in mediation of inflammatory suppression. In addition, the increased presence of the receptor in the brain of twitcher mice could represent a sign of a compensatory mechanism to the reduced presence of apelin. The up-regulation of APJ may help to adjust the effects of the reduced levels of apelin in the attempt to increase responsiveness to available apelin. Reduced apelin expression in the brain may contribute to explaining the significant weight loss of twitcher mice. Apelin has been shown to act on glucose and lipid metabolism but also to modulate insulin secretion [55]. Thus, in KD the relevance of the apelin/APJ system should be pointed out.

Regarding fatty acid metabolism, F_2-IsoPs, whose levels have been shown to be elevated in brain tissue homogenate of twitcher mice [19], are immunolocalized in brain tissue. By such detections, F_2-IsoPs were found to be progressively increased from heterozygous to homozygous condition. Thus, oxidation of arachidonic acid in the brain is also shown to occur in the heterozygous condition, when the symptoms are not present. Thus, lipid peroxidation appears to be a relevant event to the disease. Alteration in lipid metabolism/oxidation is also confirmed by the results referred to PPARγ, whose presence in brain tissue is reduced in heterozygous mice and even more in homozygous animals. Therefore, in the brain when the reduction of PPARγ occurs the oxidation of arachidonic acid increases. Since PPARγ is known to be a transcription factor involved in gene regulation of oxidative stress, lipid homeostasis and inflammation in neuropathic condition [56], the detected limited presence in brain from both heterozygous and homozygous mice appears to be linked to an increased susceptibility to lipid peroxidation and inflammation, here investigated by F_2-IsoP and RvD1. Our results on immunolocalization of PPARγ is in line with previous papers where PPARγ was detected in the cytoplasm of neurons in rat and mouse brains [57,58].

Concerning KD prevalence, males are affected as often as females [59]. In our study, both male and female mice were included accordingly. In addition, our results and our experimental experience, more than ten years, on the model [60] have not shown any difference between male and female mice.

Conclusion

In the present study, fatty acid oxidative metabolism was investigated in brain twitcher mice, a natural model of KD. A panel of specific/interrelated mediators was evaluated taking into account that arachidonic acid (fatty acid precursor of isoprostanoids), the apelin/APJ system, inflammation, and PPARγ were reported to be widely distributed in different brain regions [50,52,61,62].

Free radical-initiated fatty acid oxidation and failure of resolution of inflammation are suggested to be relevant factors in KD brain pathology: (i) lipid metabolism is deranged and oxidation of fatty acid increases; (ii) the amount of lipid mediators is related to the phenotypic manifestations of neurological impairment; (iii) lipid mediator levels are related to the severity of disease (Fig. 7). Our findings establish a new facet of the neurobiology of lipid oxidation by providing experimental support to the notion that lipid metabolism is an active player in the pathogenesis of KD. Modulation of fatty acid metabolism and lipid mediators in the brain might be proposed as a means to improve quality of life in KD.

Availability of Data and Materials

All authors had full access to all the data in the study and take responsibility for the integrity of the data and the accuracy of the data analysis. All data used to support the findings of this study are included within the article and all data are available.

Author Contributions

Conceptualization, CS, VC; Sample collection, GP, ACEG, VC; Methodology, CS, GC, GP, ACEG, EM, DN, GB, VC; Laboratory investigation, CS, GC, GP, ACEG, EM, DN, GB, VC; Manuscript draft preparation, CS, VC; Writing—review and editing, CS, GC, GP, ACEG, EM, DN, VC; Funding, VC. All authors contributed to editorial changes in the manuscript. All authors read and approved the final manuscript. All authors have participated sufficiently in the work and agreed to be accountable for all aspects of the work.

Ethics Approval and Consent to Participate

Institutional Animal Care and Use Committee approved all experimental procedures involving animals in accordance with institutional guidelines for animal care and use (Project no. 364; authorization no. 61/2022-PR).

Acknowledgment

Not applicable.

Funding

This study was partially funded by Italian Association for Leucodistrophy of Krabbe “Progetto Grazia” (grant number 20821141006/55048726).

Conflict of Interest

The authors declare no conflict of interest.

References

[1] Jain M, De Jesus O. Krabbe Disease. 2022. Available at: https://www.ncbi.nlm.nih.gov/books/NBK562315/ (Accessed: 14 December 2023).
[2] Graziano ACE, Cardile V. History, genetic, and recent advances on Krabbe disease. Gene. 2015; 555: 2–13.
[3] Cachón-González MB, Wang S, Cox TM. Expression of Ripk1 and DAM genes correlates with severity and progression of Krabbe disease. Human Molecular Genetics. 2021; 30: 2082–2099.
[4] Zaccariotto E, Cachón-González MB, Wang B, Lim S, Hirth B, Park H, *et al*. A novel brain-penetrant oral UGT8 inhibitor decreases in vivo galactosphingolipid biosynthesis in murine Krabbe disease. Biomedicine & Pharmacotherapy = Biomedecine & Pharmacotherapie. 2022; 149: 112808.
[5] Kempuraj D, Thangavel R, Natteru PA, Selvakumar GP, Saeed D, Zahoor H, *et al*. Neuroinflammation Induces Neurodegeneration. Journal of Neurology, Neurosurgery and Spine. 2016; 1: 1003.
[6] Leng F, Edison P. Neuroinflammation and microglial activation in Alzheimer disease: where do we go from here? Nature Reviews. Neurology. 2021; 17: 157–172.
[7] Potter GB, Petryniak MA. Neuroimmune mechanisms in Krabbe's disease. Journal of Neuroscience Research. 2016; 94: 1341–1348.
[8] Rafi MA. Krabbe disease: A personal perspective and hypothesis. BioImpacts: BI. 2022; 12: 3–7.
[9] Weinstock NI, Shin D, Dhimal N, Hong X, Irons EE, Silvestri NJ, *et al*. Macrophages Expressing GALC Improve Peripheral Krabbe Disease by a Mechanism Independent of Cross-Correction. Neuron. 2020; 107: 65–81.e9.
[10] Inoue K. Potential significance of CX3CR1 dynamics in stress resilience against neuronal disorders. Neural Regeneration Research. 2022; 17: 2153–2156.
[11] Ayub M, Jin HK, Bae JS. Sphingosine kinase-dependent regulation of pro-resolving lipid mediators in Alzheimer's disease. Biochimica et Biophysica Acta. Molecular and Cell Biology of Lipids. 2022; 1867: 159126.
[12] Recchiuti A, Serhan CN. Pro-Resolving Lipid Mediators (SPMs) and Their Actions in Regulating miRNA in Novel Resolution Circuits in Inflammation. Frontiers in Immunology. 2012; 3: 298.
[13] Serhan CN. Pro-resolving lipid mediators are leads for resolution physiology. Nature. 2014; 510: 92–101.
[14] Ferreira I, Falcato F, Bandarra N, Rauter AP. Resolvins, Protectins, and Maresins: DHA-Derived Specialized Pro-Resolving Mediators, Biosynthetic Pathways, Synthetic Approaches, and Their Role in Inflammation. Molecules (Basel, Switzerland). 2022; 27: 1677.
[15] Bazan NG. Neuroprotectin D1 (NPD1): a DHA-derived mediator that protects brain and retina against cell injury-induced oxidative stress. Brain Pathology (Zurich, Switzerland). 2005; 15: 159–166.
[16] Chiang N, Serhan CN. Specialized pro-resolving mediator network: an update on production and actions. Essays in Biochemistry. 2020; 64: 443–462.
[17] Milne GL, Dai Q, Roberts LJ, 2nd. The isoprostanes–25 years later. Biochimica et Biophysica Acta. 2015; 1851: 433–445.
[18] Basu S. Bioactive eicosanoids: role of prostaglandin F(2α) and F_2-isoprostanes in inflammation and oxidative stress related pathology. Molecules and Cells. 2010; 30: 383–391.
[19] Signorini C, Cardile V, Pannuzzo G, Graziano ACE, Durand T, Galano JM, *et al*. Increased isoprostanoid levels in brain from murine model of Krabbe disease - Relevance of isoprostanes, dihomo-isoprostanes and neuroprostanes to disease severity. Free Radical Biology & Medicine. 2019; 139: 46–54.
[20] Quintão NLM, Santin JR, Stoeberl LC, Corrêa TP, Melato J, Costa R. Pharmacological Treatment of Chemotherapy-Induced Neuropathic Pain: PPARγ Agonists as a Promising Tool. Frontiers in Neuroscience. 2019; 13: 907.
[21] Wang X, Zhang L, Li P, Zheng Y, Yang Y, Ji S. Apelin/APJ system in inflammation. International Immunopharmacology. 2022; 109: 108822.
[22] Wan T, Fu M, Jiang Y, Jiang W, Li P, Zhou S. Research Progress on Mechanism of Neuroprotective Roles of Apelin-13 in Prevention and Treatment of Alzheimer's Disease. Neurochemical Research. 2022; 47: 205–217.
[23] Angelopoulou E, Paudel YN, Bougea A, Piperi C. Impact of the apelin/APJ axis in the pathogenesis of Parkinson's disease with therapeutic potential. Journal of Neuroscience Research. 2021; 99: 2117–2133.
[24] Jiang Y, Wang S, Liu X. Low serum apelin levels are associated with mild cognitive impairment in Type 2 diabetic patients. BMC Endocrine Disorders. 2022; 22: 137.
[25] Zhou Q, Cao J, Chen L. Apelin/APJ system: A novel therapeutic target for oxidative stress-related inflammatory diseases (Review). International Journal of Molecular Medicine. 2016; 37: 1159–1169.
[26] Zhou JX, Shuai NN, Wang B, Jin X, Kuang X, Tian SW. Neuroprotective gain of Apelin/APJ system. Neuropeptides. 2021; 87: 102131.
[27] He S, Li J, Wang J, Zhang Y. Hypoxia exposure alleviates impaired muscular metabolism, glucose tolerance, and aerobic capacity in apelin-knockout mice. FEBS Open Bio. 2019; 9: 498–509.
[28] Yan J, Wang A, Cao J, Chen L. Apelin/APJ system: an emerging therapeutic target for respiratory diseases. Cellular and Molecular Life Sciences: CMLS. 2020; 77: 2919–2930.
[29] Huang Z, Luo X, Liu M, Chen L. Function and regulation of apelin/APJ system in digestive physiology and pathology. Journal of Cellular Physiology. 2019; 234: 7796–7810.
[30] Lv SY, Yang YJ, Chen Q. Regulation of feeding behavior, gastrointestinal function and fluid homeostasis by apelin. Peptides. 2013; 44: 87–92.
[31] Suzuki K, Suzuki K. The twitcher mouse: a model for Krabbe disease and for experimental therapies. Brain Pathology (Zurich, Switzerland). 1995; 5: 249–258.
[32] De Felice C, Della Ragione F, Signorini C, Leoncini S, Pecorelli A, Ciccoli L, *et al*. Oxidative brain damage in Mecp2-mutant murine models of Rett syndrome. Neurobiology of Disease. 2014; 68: 66–77.
[33] Micheli L, Collodel G, Moretti E, Noto D, Menchiari A, Cerretani D, *et al*. Redox imbalance induced by docetaxel in the neuroblastoma SH-SY5Y cells: a study of docetaxel-induced neuronal damage. Redox Report: Communications in Free Radical Research. 2021; 26: 18–28.
[34] Stafforini DM, Sheller JR, Blackwell TS, Sapirstein A, Yull FE, McIntyre TM, *et al*. Release of free F2-isoprostanes from esterified phospholipids is catalyzed by intracellular and plasma platelet-activating factor acetylhydrolases. The Journal of Biological Chemistry. 2006; 281: 4616–4623.
[35] Kuksis A, Pruzanski W. Hydrolysis of Phosphatidylcholine-Isoprostanes (PtdCho-IP) by Peripheral Human Group IIA, V and X Secretory Phospholipases A_2 (sPLA_2). Lipids. 2017; 52: 477–488.
[36] Signorini C, De Felice C, Durand T, Galano JM, Oger C, Leoncini S, *et al*. Isoprostanoid Plasma Levels Are Relevant to Cerebral Adrenoleukodystrophy Disease. Life (Basel, Switzerland). 2022; 12: 146.
[37] Boyd RJ, Avramopoulos D, Jantzie LL, McCallion AS. Neuroinflammation represents a common theme amongst genetic and en-

vironmental risk factors for Alzheimer and Parkinson diseases. Journal of Neuroinflammation. 2022; 19: 223.

[38] Cachón-González MB, Zhao C, Franklin RJ, Cox TM. Upregulation of non-canonical and canonical inflammasome genes associates with pathological features in Krabbe disease and related disorders. Human Molecular Genetics. 2023; 32: 1361–1379.

[39] Meroni E, Stakenborg N, Viola MF, Boeckxstaens GE. Intestinal macrophages and their interaction with the enteric nervous system in health and inflammatory bowel disease. Acta Physiologica (Oxford, England). 2019; 225: e13163.

[40] Herold K, Mrowka R. Inflammation-Dysregulated inflammatory response and strategies for treatment. Acta Physiologica (Oxford, England). 2019; 226: e13284.

[41] Chiang N, Riley IR, Dalli J, Rodriguez AR, Spur BW, Serhan CN. New maresin conjugates in tissue regeneration pathway counters leukotriene D_4-stimulated vascular responses. FASEB Journal: Official Publication of the Federation of American Societies for Experimental Biology. 2018; 32: 4043–4052.

[42] Norris PC, Skulas-Ray AC, Riley I, Richter CK, Kris-Etherton PM, Jensen GL, *et al*. Identification of specialized pro-resolving mediator clusters from healthy adults after intravenous low-dose endotoxin and omega-3 supplementation: a methodological validation. Scientific Reports. 2018; 8: 18050.

[43] Norris PC, Skulas-Ray AC, Riley I, Richter CK, Kris-Etherton PM, Jensen GL, *et al*. Author Correction: Identification of specialized pro-resolving mediator clusters from healthy adults after intravenous low-dose endotoxin and omega-3 supplementation: a methodological validation. Scientific Reports. 2019; 9: 19816.

[44] Petermann AB, Reyna-Jeldes M, Ortega L, Coddou C, Yévenes GE. Roles of the Unsaturated Fatty Acid Docosahexaenoic Acid in the Central Nervous System: Molecular and Cellular Insights. International Journal of Molecular Sciences. 2022; 23: 5390.

[45] Layé S, Nadjar A, Joffre C, Bazinet RP. Anti-Inflammatory Effects of Omega-3 Fatty Acids in the Brain: Physiological Mechanisms and Relevance to Pharmacology. Pharmacological Reviews. 2018; 70: 12–38.

[46] Bisicchia E, Sasso V, Catanzaro G, Leuti A, Besharat ZM, Chiacchiarini M, *et al*. Resolvin D1 Halts Remote Neuroinflammation and Improves Functional Recovery after Focal Brain Damage Via ALX/FPR2 Receptor-Regulated MicroRNAs. Molecular Neurobiology. 2018; 55: 6894–6905.

[47] Mostafa DG, Satti HH. Resolvin D1 Prevents the Impairment in the Retention Memory and Hippocampal Damage in Rats Fed a Corn Oil-Based High Fat Diet by Upregulation of Nrf2 and Downregulation and Inactivation of p^{66}Shc. Neurochemical Research. 2020; 45: 1576–1591.

[48] Mizwicki MT, Liu G, Fiala M, Magpantay L, Sayre J, Siani A, *et al*. 1α,25-dihydroxyvitamin D3 and resolvin D1 retune the balance between amyloid-β phagocytosis and inflammation in Alzheimer's disease patients. Journal of Alzheimer's Disease: JAD. 2013; 34: 155–170.

[49] Krashia P, Cordella A, Nobili A, La Barbera L, Federici M, Leuti A, *et al*. Blunting neuroinflammation with resolvin D1 prevents early pathology in a rat model of Parkinson's disease. Nature Communications. 2019; 10: 3945.

[50] Villapol S. Roles of Peroxisome Proliferator-Activated Receptor Gamma on Brain and Peripheral Inflammation. Cellular and Molecular Neurobiology. 2018; 38: 121–132.

[51] Iacono D, Koga S, Peng H, Manavalan A, Daiker J, Castanedes-Casey M, *et al*. Galactosylceramidase deficiency and pathological abnormalities in cerebral white matter of Krabbe disease. Neurobiology of Disease. 2022; 174: 105862.

[52] Nathan C. Nonresolving inflammation redux. Immunity. 2022; 55: 592–605.

[53] Lv SY, Chen WD, Wang YD. The Apelin/APJ System in Psychosis and Neuropathy. Frontiers in Pharmacology. 2020; 11: 320.

[54] Kidoya H, Naito H, Takakura N. Apelin induces enlarged and nonleaky blood vessels for functional recovery from ischemia. Blood. 2010; 115: 3166–3174.

[55] Bertrand C, Valet P, Castan-Laurell I. Apelin and energy metabolism. Frontiers in Physiology. 2015; 6: 115.

[56] Zhang M, Hu M, Alles SRA, Montera MA, Adams I, Santi MD, *et al*. Peroxisome proliferator-activated receptor gamma agonist ELB00824 suppresses oxaliplatin-induced pain, neuronal hypersensitivity, and oxidative stress. Neuropharmacology. 2022; 218: 109233.

[57] Moreno S, Farioli-Vecchioli S, Cerù MP. Immunolocalization of peroxisome proliferator-activated receptors and retinoid X receptors in the adult rat CNS. Neuroscience. 2004; 123: 131–145.

[58] Warden A, Truitt J, Merriman M, Ponomareva O, Jameson K, Ferguson LB, *et al*. Localization of PPAR isotypes in the adult mouse and human brain. Scientific Reports. 2016; 6: 27618.

[59] Sadovnick AD. Multiple Sclerosis and Other Demyelinating Disorders. In: Rimoin D, Pyeritz R, Korf B, eds. Emery and Rimoin's Principles and Practice of Medical Genetics. 6th edn. Academic Press: Cambridge. 2013: 1–8.

[60] Pannuzzo G, Cardile V, Costantino-Ceccarini E, Alvares E, Mazzone D, Perciavalle V. A galactose-free diet enriched in soy isoflavones and antioxidants results in delayed onset of symptoms of Krabbe disease in twitcher mice. Molecular Genetics and Metabolism. 2010; 100: 234–240.

[61] Xiao Y, Huang Y, Chen ZY. Distribution, depletion and recovery of docosahexaenoic acid are region-specific in rat brain. The British Journal of Nutrition. 2005; 94: 544–550.

[62] De Mota N, Lenkei Z, Llorens-Cortès C. Cloning, pharmacological characterization and brain distribution of the rat apelin receptor. Neuroendocrinology. 2000; 72: 400–407.